



<http://www.diva-portal.org>

Postprint

This is the accepted version of a paper published in *Applied Physics Letters*. This paper has been peer-reviewed but does not include the final publisher proof-corrections or journal pagination.

Citation for the original published paper (version of record):

Jablonka, L., Kubart, T., Gustavsson, F., Descoins, M., Mangelinck, D. et al. (2018)  
Improving the morphological stability of nickel germanide by tantalum and tungsten additions  
*Applied Physics Letters*, 112(10)  
<https://doi.org/10.1063/1.5019440>

Access to the published version may require subscription.

N.B. When citing this work, cite the original published paper.

Permanent link to this version:

<http://urn.kb.se/resolve?urn=urn:nbn:se:uu:diva-344676>

# Improving the morphological stability of nickel germanide by tantalum and tungsten additions

L. Jablonka,<sup>1</sup> T. Kubart,<sup>1</sup> F. Gustavsson,<sup>1,a)</sup> M. Descoins,<sup>2</sup> D. Mangelinck,<sup>2</sup> S.-L. Zhang,<sup>1</sup> and Z. Zhang<sup>1,b)</sup>

<sup>1</sup>*Solid State Electronics, The Ångström Laboratory, Uppsala University, SE-75121 Uppsala, Sweden*

<sup>2</sup>*IM2NP, CNRS-Université d'Aix-Marseille, Case 142, 13397 Marseille Cedex 20, France*

To enhance the morphological stability of NiGe, a material of interest as source drain-contacts in Ge-based field effect transistors, Ta or W is added as either interlayer or capping layer. The efficacy of this Ta or W addition is evaluated with pure NiGe as a reference. While interlayers increase the NiGe formation temperature, capping layers do not retard the NiGe formation. Regardless of the initial position of Ta or W, the morphological stability of NiGe against agglomeration can be improved by up to 100 °C. The improved thermal stability can be ascribed to an inhibited surface diffusion, owing to Ta or W being located on top of NiGe after annealing, as confirmed by means of transmission electron microscopy, Rutherford backscattering spectrometry, and atom probe tomography. The latter also shows a 0.3 at. % solubility of Ta in NiGe at 450 °C, while no such incorporation of W is detectable.

---

<sup>a</sup>current address: Swerea KIMAB AB, Box 7047, SE-16407 Kista, Sweden

<sup>b</sup>zhen.zhang@angstrom.uu.se

Germanium has been considered as a replacement for Si in metal-oxide-semiconductor field effect transistor (MOSFET) channels,<sup>1-4</sup> because of its higher carrier mobilities and lower processing temperatures. The lower processing temperatures also make Ge an especially interesting candidate for the upper-tier device layers in monolithically integrated three-dimensional circuits as an example.<sup>5</sup> Nickel germanide is studied as a material for contact metallization of the source and drain terminals of a Ge-MOSFET, owing to its low resistivity and compatibility with a self-aligned process.<sup>6,7</sup> The formation of the desired low-resistivity phase NiGe usually occurs via the high-resistivity, metal-rich phase  $\epsilon$ -Ni<sub>5</sub>Ge<sub>3</sub><sup>8-10</sup> and NiGe is also the last phase to form. The applicability of thin NiGe layers, however, is limited by the tendency to agglomerate (*i.e.* to break up into islands) at lower temperatures than its NiSi counterpart in Si-MOSFETs.<sup>10</sup> Agglomeration degrades the electrical connectivity and can thereby cause contact failures. Since the driving force for agglomeration is the minimization of the total free energy by eliminating grain boundaries and minimizing interfaces,<sup>11-13</sup> thinner NiGe layers tend to agglomerate at even lower temperatures.<sup>10</sup> Enlarging the process temperature window by suppressing agglomeration is thus important for the integration of NiGe into future down-scaled Ge-based CMOS technology nodes.

Previous efforts to suppress the agglomeration of thin NiGe layers focused on either the addition of metals or on modifying the Ge substrate. The addition of alloying elements including Pt (from an alloyed target with 1 at.% Pt<sup>14</sup> or using co-sputtering resulting in Pt contents of 0 to 20 at.%<sup>15</sup>) or Pd (layered structure of 2 nm Pd and 10 nm Ni<sup>16</sup>) stabilized the layers as a result of the formation of respective ternary germanides by 50 to 100 °C. These ternary germanide alloys have higher melting points and possess larger (absolute) Gibbs free energies from the effect of mixing than pure NiGe. The alloying with Zr<sup>17,18</sup> or Ti<sup>19</sup> was proven to be equally effective, but due to the formation of Zr or Ti-rich capping layers after annealing. On amorphous Ge-substrates, NiGe was shown to agglomerate at a higher

temperature compared to on crystalline Ge, due to missing destabilizing effects of axiotaxial textures.<sup>20</sup> In the present study, the influence of adding Ta or W to the system of Ni and Ge prior to annealing is investigated. Tantalum and W have been selected because they do not form germanides below 700 and 900 °C, respectively.<sup>6</sup> Both Ta and W diffuse more slowly than Ge and Ni, hence their use as markers for studying the reactive diffusion in Ni/Ge was reported in previous studies.<sup>21</sup> Such slow-diffusing species tend to segregate at interfaces as well as at grain boundaries and can thereby inhibit the agglomeration.<sup>22</sup> Apart from this, the formation of ternary phases or alloys with Ni and Ge is unlikely with both Ta and W. For Ta, a rise in agglomeration temperature by 50 °C was reported when co-depositing Ni and Ta on Ge.<sup>23</sup> However, the 30 nm thick Ni layers used in ref. <sup>23</sup> are too thick to be relevant for the integration in future down-scaled devices. A reported beneficial property of W is its capability of reducing the Ge out-diffusion on patterned substrates when implanted into NiGe.<sup>24</sup>

In this study, 2.2 μm thick Ge layers were epitaxially grown on (100) Si-on-insulator substrates.<sup>25</sup> Prior to metal deposition, the substrates were cleaned using a solution of H<sub>2</sub>O<sub>2</sub>/NH<sub>4</sub>OH/H<sub>2</sub>O at a ratio of 1/1/5000 for 60 s followed by a 40 s dip in 0.5 % HF.<sup>26</sup> All metal depositions were carried out by magnetron sputtering at a pressure of 4.5 mTorr and with an Ar flow of 40 sccm. Nickel was deposited with an RF power of 150 W. Tantalum and W were deposited using a pulsed DC process with a pulse-off time of 0.5 μs, a pulse frequency of 250 kHz and at 45 W. No intentional substrate heating was used. The Ni thicknesses ranged from 5 to 12 nm, while Ta or W was deposited as an interlayer or a capping layer with thicknesses ranging from 0.2 to 3 nm without breaking the vacuum. The amounts of deposits were controlled by deposition time and calibrated by means of Rutherford backscattering spectrometry (RBS) using alpha particles at an energy of 2 MeV and a scattering angle of 170°. To avoid channeling through the substrate during RBS measurements, the incident angle of the ion beam was -5° off the substrate normal and the

sample tilt was changed randomly within  $1^\circ$ . After the deposition, the substrates were sliced into pieces of 1.5 cm by 2.0 cm and annealed to temperatures ranging from 150 to 650  $^\circ\text{C}$  in nitrogen atmosphere using rapid thermal processing (RTP) with a ramp rate of 10  $^\circ\text{C}/\text{s}$  and a soaking time of 30 s. The sheet resistance,  $R_{\text{sh}}$ , was measured before and after the depositions as well as after the RTP using a four-point probe setup. Selected samples were furthermore analyzed using scanning electron microscopy (SEM), transmission electron microscopy (TEM), and atom probe tomography (APT).

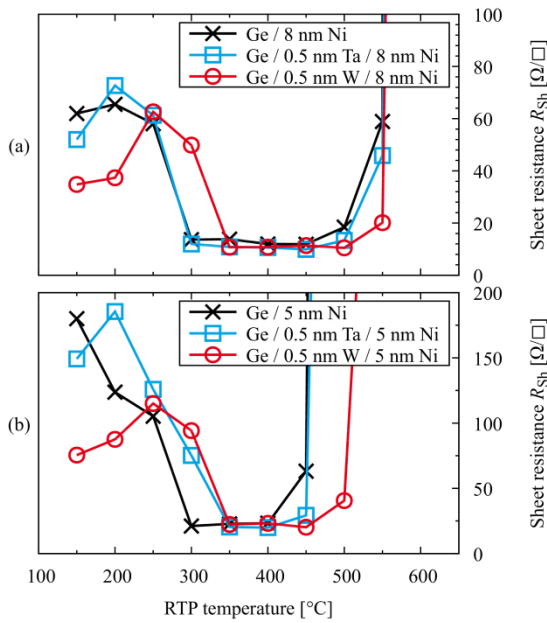


FIG. 1 Dependence of the sheet resistance on the RTP temperature after addition of 0.5 nm Ta or W interlayer to (a) 8 nm Ni, and (b) 5 nm Ni.

The addition of Ta or W as an interlayer between Ge and Ni is found to affect the process temperature window of NiGe, which corresponds to the temperature range where the lowest  $R_{\text{sh}}$  can be measured, see FIGs. 1 and 2. The process temperature window is limited by the completion of the NiGe formation at its lower end and by the beginning of agglomeration at the upper end. Both ends are influenced by the initial Ni thickness (FIG. 1) and the interlayer thickness (FIG. 2). In FIG. 1(a), when a 0.5 nm Ta or W interlayer is added to 8 nm of Ni,  $R_{\text{sh}}$  is seen to first increase and then to decrease between 150 and 300  $^\circ\text{C}$  at which reactive

diffusion takes place between Ni and Ge. Nickel, the dominant diffusing species during the initial formation of  $\text{Ni}_5\text{Ge}_3$ ,<sup>21</sup> needs to diffuse through the Ta or W interlayer in order to react with Ge. The high  $R_{\text{sh}}$  is thus caused by the formation of the high-resistivity phase  $\text{Ni}_5\text{Ge}_3$  from the Ni layer of much lower resistivity and the Ge-substrate. With pure Ni as well as with a Ta interlayer, the highest  $R_{\text{sh}}$  is observed at 200 °C while it occurs at 250 °C with a W interlayer. Similarly, the temperature for completing the NiGe formation is 300 °C for pure Ni as well as for the Ta interlayer samples, whereas with W the NiGe formation is not completed until the temperature is increased to 350 °C. For 12 nm Ni, the same behavior as in FIG. 1(a) has been observed (data not shown). The observed higher temperatures for the formation of  $\text{Ni}_5\text{Ge}_3$  and NiGe with the W interlayer indicate that W blocks the Ni diffusion more efficiently than Ta does. At the given annealing conditions with fixed ramp rates and soaking times, the delayed  $\text{Ni}_5\text{Ge}_3$  formation leads to a raised temperature for completing the NiGe formation. For example, compared to 250 °C, the  $R_{\text{sh}}$  of the W interlayer sample at 300 °C is reduced which indicates that the NiGe formation may already have started, but is far from being completed. The beginning of agglomeration is indicated by the rise in  $R_{\text{sh}}$  and occurs at 500 °C when pure Ni is used, but at 550 °C when a Ta or W interlayer is added.

In FIG. 1(b), when a thinner Ni layer of 5 nm is used, the temperature of complete NiGe formation is increased to 350 °C for the Ta interlayer case. Compared to using 8 nm Ni and a Ta interlayer this is an increase of 50 °C, which can be explained by the formation of NiGe from  $\text{Ni}_5\text{Ge}_3$  becoming nucleation-controlled as reported earlier.<sup>10</sup> The critical  $\text{Ni}_5\text{Ge}_3$  thickness above which NiGe would spontaneously grow was estimated to be 8.3 nm (corresponding to 4.7 nm of unreacted Ni);<sup>8,10,27</sup> below this thickness, the nucleation of NiGe requires a higher temperature. Comparing the sample with 5 nm Ni and Ta to the pure 5 nm Ni case, however, the temperature of complete NiGe formation is increased by 50 °C as well.

This suggests that the complete NiGe formation is delayed by a combination of an inhibited Ni diffusion through the Ta interlayer and a nucleation-controlled NiGe formation.

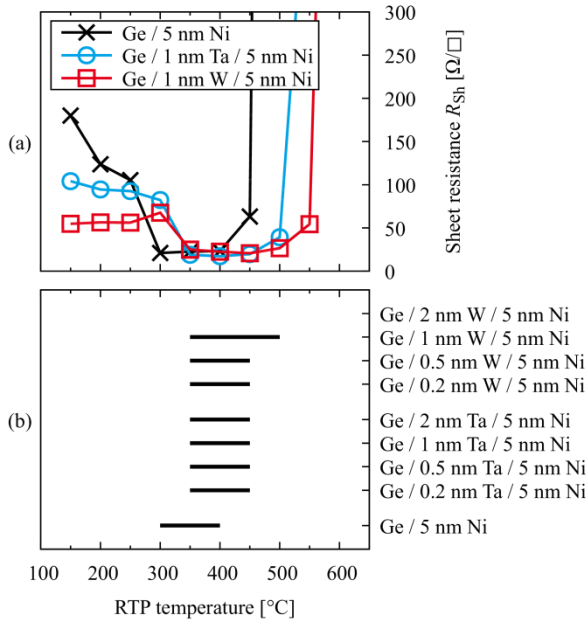


FIG. 2 (a) Dependence of the sheet resistance on the RTP temperature for 5 nm Ni samples. With added Ta and W interlayers, the complete NiGe formation is delayed to higher temperature by 50  $^{\circ}\text{C}$ . The agglomeration of NiGe layers is suppressed by the presence of Ta and W. (b) Horizontal bars for the process temperature windows in which non-agglomerated NiGe is formed, *i.e.* when the sheet resistance does not exceed 150 % of its minimum value.

When the interlayer thickness is increased to 1 nm while the Ni layer is kept at 5 nm, the temperature of complete NiGe formation is similarly shifted to 350  $^{\circ}\text{C}$  for both Ta and W as shown in FIG. 2(a). However, using thicker Ta or W interlayers improves the resistance to agglomeration of the NiGe. In FIG. 2(b), the process temperature windows for the formation of morphologically stable NiGe layers from 5 nm Ni are depicted as horizontal bars for interlayer thicknesses between 0.2 and 2 nm. Here, the layers were defined as morphologically stable when  $R_{sh}$  does not exceed 150 % of its minimum value. A change in interlayer thickness does not change the temperature of complete NiGe formation except when a 2 nm W interlayer is used, see FIG. 2(b); NiGe is not fully formed even after a prolonged annealing at 450  $^{\circ}\text{C}$  for 120 s (data not shown). Hereby, the observation that W

inhibits the Ni diffusion more efficiently than Ta is further supported. The upper end of the process temperature window, however, requires further scrutiny and is discussed below.

In brief, a Ta or W interlayer causes the NiGe agglomeration temperature to increase by 50 to 100 °C for all studied thicknesses, see FIGs. 1 and 2, wherein the 1 nm W case leads to the most stable NiGe layers. The TEM micrographs in FIGs. 3(a) and 4(a)-(b), the APT data in FIGs. 3(b) and 4(c), and the RBS results (not shown here) confirm that the Ta or W layer initially located close to the Ge substrate is present on top of the formed NiGe layers after annealing, thereby affirming the predominant Ni diffusion during the reaction. It is plausible that the surface Ta or W decelerates the Ni surface diffusion and thus helps to stabilize the NiGe layers against agglomeration.

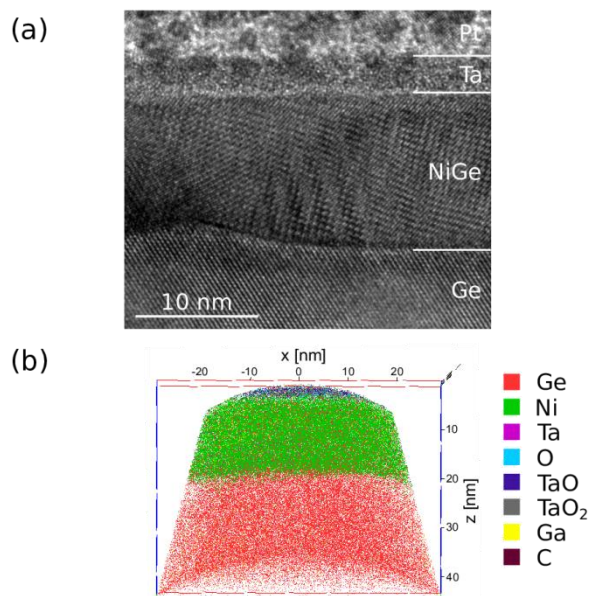


FIG. 3 (a) Cross-sectional TEM image of Ge / 0.5 nm Ta / 5 nm Ni after RTP at 400 °C. (b) Reconstructed APT data of Ge / 1 nm Ta / 5 nm Ni after RTP at 450 °C.

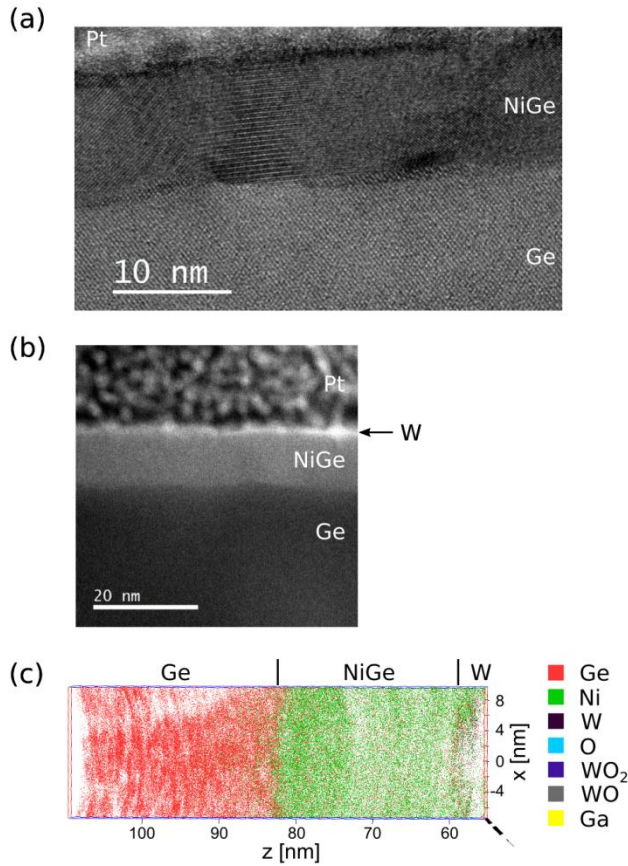


FIG. 4 (a) Cross-sectional TEM image of Ge / 0.5 nm W / 5 nm Ni after RTP at 400 °C. (b) High-angle annular dark-field STEM of the same sample. (c) Clip of reconstructed APT data of Ge / 1 nm W / 5 nm Ni after RTP at 450 °C.

Apart from the observation of Ta or W being located on the surface, Ta or W could also be present in the NiGe grain boundaries. Unfortunately, the prepared APT samples do not contain any grain-boundaries for such a study. Nevertheless, Ta is found to be uniformly distributed within the NiGe layer formed after a 450 °C anneal of the sample with a 1 nm Ta interlayer and 5 nm Ni. The atomic composition is determined to be  $\text{Ni}_{1.0}\text{Ge}_{1.0}\text{Ta}_{0.003}$ , see FIG. 3(b) for the reconstructed atom probe data. This result indicates a solubility of Ta in NiGe of 0.3 at.% at 450 °C. In an otherwise comparable sample with a 1 nm W interlayer, no W lattice incorporation in the NiGe can be concluded within the detection limit of APT, see FIG. 4(c). Even though a W concentration of 0.2 at.% is indicated by the APT analysis software, no W peaks are present above the noise in the mass spectrum. Compared to the aforementioned incorporation of Pt or Pd, the Ta content in NiGe is very low. Consequently, a significant effect of Ta lattice incorporation on the morphological stability of NiGe is

unlikely. Neither Ta nor W is found at the Ge/NiGe-interface, which is expected as a result of Ni being the dominant diffusion species during the  $\text{Ni}_5\text{Ge}_3$  formation; the subsequent NiGe formation would just proceed beneath the surface Ta or W.

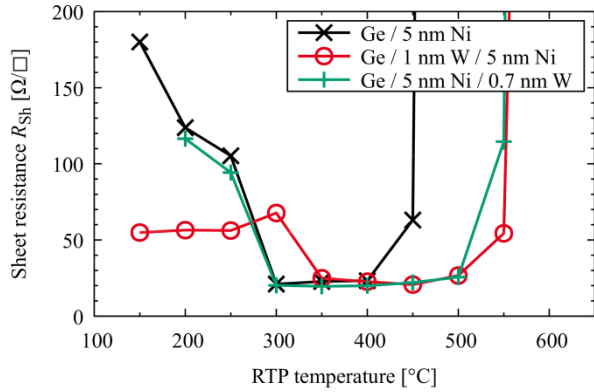


FIG. 5 Comparison between a 1 nm W interlayer and a 0.7 nm W capping layer for the Ni-germanide formation with a 5 nm Ni layer.

While the agglomeration of NiGe layers is shown to be inhibited due to Ta or W being moved to the NiGe surface after annealing, the disadvantage of the interlayer configuration is a raised temperature for completing the NiGe formation, which reduces the process temperature window. Capping Ta or W layers are therefore used to evaluate their efficacy in expanding the NiGe process temperature window. Since W shows better results than Ta in stabilizing the formed NiGe layers, the focus is placed on the W capping layer and the results are depicted in FIG. 5. As expected, both the interlayer and capping layer configurations lead to the same improvements with respect to increasing the agglomeration temperature despite a difference in W thickness of 0.3 nm. The temperature of complete NiGe formation, however, is unaffected in the presence of the W capping layer as compared to the pure Ni reference. As seen in FIG. 2(b), a 0.3 nm difference in W interlayer thickness would not alter the NiGe formation temperature and the comparison in FIG. 5 is hence valid. Thus, the largest extension of the process temperature window for an initial Ni thickness of 5 nm is 100 °C and obtained with a 0.7 nm W capping layer.

To summarize, the process temperature window of NiGe layers formed from initial Ni thicknesses from 5 to 12 nm could be modified by the addition of Ta or W layers. Whether these layers were added as interlayer or capping layer did not influence the agglomeration temperature, since Ta or W was always found to be located on top of the NiGe layers after annealing. The temperature of complete NiGe formation, however, was increased by 50 °C with the interlayer scheme while it remained unchanged with a capping layer scheme. The largest extension of the process temperature window of 100 °C was observed when a 0.7 nm thick W capping layer was used. The suppressed agglomeration most likely arose from a decelerated surface diffusion, since it was found independent of the initial Ni thickness. It is worth noting that a minute amount of Ta was incorporated into the NiGe lattice, while W was not.

Per-Erik Hellström and Ahmad Abedin are acknowledged for preparing the Ge substrates. Financial support by the Swedish Foundation for Strategic Research (SSF) via contract SE13-0033 is acknowledged. The RBS measurements were supported by SSF via contract RIF14-0053 as well as by the Swedish Research Council via VR-RFI contract C0514401. The APT measurements were made possible by funding from the French CNRS (FR3507) and CEA METSA network ([www.metsa.fr](http://www.metsa.fr)). L.J. would like to thank the Stenholm, Wilgott Travel Scholarship for financing travel costs to Marseille.

<sup>1</sup> C.O. Chui, H. Kim, D. Chi, B.B. Triplett, P.C. McIntyre, and K.C. Saraswat, in *Int. Electron Devices Meet. Tech. Dig.* (2002), pp. 437–440.

<sup>2</sup> H. Shang, H. Okorn-Schmidt, K.K. Chan, M. Copel, J.A. Ott, P.M. Kozlowski, S.E. Steen, S.A. Cordes, H.S.P. Wong, E.C. Jones, and W.E. Haensch, in *Int. Electron Devices Meet. Tech. Dig.* (2002), pp. 441–444.

<sup>3</sup> C.O. Chui, F. Ito, and K.C. Saraswat, *IEEE Trans. Electron Devices* **53**, 1501 (2006).

<sup>4</sup> K. Saraswat, C.O. Chui, T. Krishnamohan, D. Kim, A. Nayfeh, and A. Pethe, *Mater. Sci. Eng. B* **135**, 242 (2006).

<sup>5</sup> P. Batude, M. Vinet, A. Pouydebasque, C. Le Royer, B. Previtali, C. Tabone, L. Clavelier, S. Michaud, A. Valentian, O. Thomas, O. Rozeau, P. Coudrain, C. Leyris, K. Romanjek, X. Garros, L. Sanchez, L. Baud, A. Roman, V. Carron, H. Grampeix, E. Augendre, A. Toffoli, F.

- Allain, P. Grosgeorges, V. Mazzochi, L. Tosti, F. Andrieu, J.-M. Hartmann, D. Lafond, S. Deleonibus, and O. Faynot, in *2009 Symp. VLSI Technol.* (2009), pp. 166–167.
- <sup>6</sup> S. Gaudet, C. Detavernier, A.J. Kellock, P. Desjardins, and C. Lavoie, *J. Vac. Sci. Technol. A* **24**, 474 (2006).
- <sup>7</sup> D.P. Brunco, K. Opsomer, B.D. Jaeger, G. Winderickx, K. Verheyden, and M. Meuris, *Electrochem. Solid-State Lett.* **11**, H39 (2008).
- <sup>8</sup> F. Nemouchi, D. Mangelinck, C. Bergman, G. Clugnet, P. Gas, and J.L. Lábár, *Appl. Phys. Lett.* **89**, 131920 (2006).
- <sup>9</sup> B. De Schutter, K.V. Stiphout, N.M. Santos, E. Bladt, J. Jordan-Sweet, S. Bals, C. Lavoie, C.M. Comrie, A. Vantomme, and C. Detavernier, *J. Appl. Phys.* **119**, 135305 (2016).
- <sup>10</sup> L. Jablonka, T. Kubart, D. Primetzhofer, A. Abedin, P.-E. Hellström, M. Östling, J. Jordan-Sweet, C. Lavoie, S.-L. Zhang, and Z. Zhang, *J. Vac. Sci. Technol. B* **35**, 020602 (2017).
- <sup>11</sup> S.-L. Zhang and M. Östling, *Crit. Rev. Solid State Mater. Sci.* **28**, 1 (2003).
- <sup>12</sup> C.V. Thompson, *Annu. Rev. Mater. Res.* **42**, 399 (2012).
- <sup>13</sup> S.-L. Zhang and Z. Zhang, in *Met. Films Electron. Opt. Magn. Appl.*, edited by K. Barmak and K. Coffey (Woodhead Publishing, Sawston, 2014), pp. 244–301.
- <sup>14</sup> Y.-Y. Zhang, J. Oh, S.-G. Li, S.-Y. Jung, K.-Y. Park, G.-W. Lee, P. Majhi, H.-H. Tseng, R. Jammy, and H.-D. Lee, *IEEE Trans. Nanotechnol.* **9**, 258 (2010).
- <sup>15</sup> M.-H. Kang, H.-S. Shin, J.-H. Yoo, G.-W. Lee, J.-W. Oh, P. Majhi, R. Jammy, and H.-D. Lee, *IEEE Trans. Nanotechnol.* **11**, 769 (2012).
- <sup>16</sup> Y.-Y. Zhang, C.-J. Choi, J. Oh, I.-S. Han, S.-G. Li, K.-Y. Park, H.-S. Shin, G.-W. Lee, J.-S. Wang, P. Majhi, R. Jammy, and H.-D. Lee, *Electrochem. Solid-State Lett.* **12**, H402 (2009).
- <sup>17</sup> S.L. Liew, R.T.P. Lee, K.Y. Lee, B. Balakrisnan, S.Y. Chow, M.Y. Lai, and D.Z. Chi, *Thin Solid Films* **504**, 104 (2006).
- <sup>18</sup> J.-W. Lee, J.-H. Bae, J.-H. Hwang, H.-K. Kim, M.-H. Park, H. Kim, and C.-W. Yang, *Microelectron. Eng.* **89**, 23 (2012).
- <sup>19</sup> S. Zhu, M.B. Yu, G.Q. Lo, and D.L. Kwong, *Appl. Phys. Lett.* **91**, 051905 (2007).
- <sup>20</sup> K. van Stiphout, F.A. Geenen, B.D. Schutter, N.M. Santos, S.M.C. Miranda, V. Joly, C. Detavernier, L.M.C. Pereira, K. Temst, and A. Vantomme, *J. Phys. Appl. Phys.* **50**, 455301 (2017).
- <sup>21</sup> C.M. Comrie, D. Smeets, K.J. Pondo, C. van der Walt, J. Demeulemeester, W. Knaepen, C. Detavernier, A. Habanyama, and A. Vantomme, *Thin Solid Films* **526**, 261 (2012).
- <sup>22</sup> M. Bouville, D. Chi, and D.J. Srolovitz, *Phys. Rev. Lett.* **98**, 085503 (2007).
- <sup>23</sup> K. Park, B.H. Lee, D. Lee, D.-H. Ko, K.H. Kwak, C.-W. Yang, and H. Kim, *J. Electrochem. Soc.* **154**, H557 (2007).
- <sup>24</sup> V. Carron, F. Nemouchi, F. Milesi, Y. Morand, P. Batude, L. Hutin, and C. Le Royer, in *2014 Int. Workshop Junction Technol. IWJT* (2014), pp. 1–6.
- <sup>25</sup> A. Abedin, A. Asadollahi, K. Garidis, P.-E. Hellström, and M. Ostling, *ECS Trans.* **75**, 615 (2016).
- <sup>26</sup> D.P. Brunco, B.D. Jaeger, G. Eneman, J. Mitard, G. Hellings, A. Satta, V. Terzieva, L. Souriau, F.E. Leys, G. Pourtois, M. Houssa, G. Winderickx, E. Vrancken, S. Sioncke, K. Opsomer, G. Nicholas, M. Caymax, A. Stesmans, J.V. Steenbergen, P.W. Mertens, M. Meuris, and M.M. Heyns, *J. Electrochem. Soc.* **155**, H552 (2008).
- <sup>27</sup> F. Nemouchi, D. Mangelinck, J.L. Lábár, M. Putero, C. Bergman, and P. Gas, *Microelectron. Eng.* **83**, 2101 (2006).